VOLUME 33 | SUPPLEMENT 2 | MARCH 2020

MODERN PATHOLOGY

ABSTRACTS

INFECTIOUS DISEASE PATHOLOGY (1503-1521)

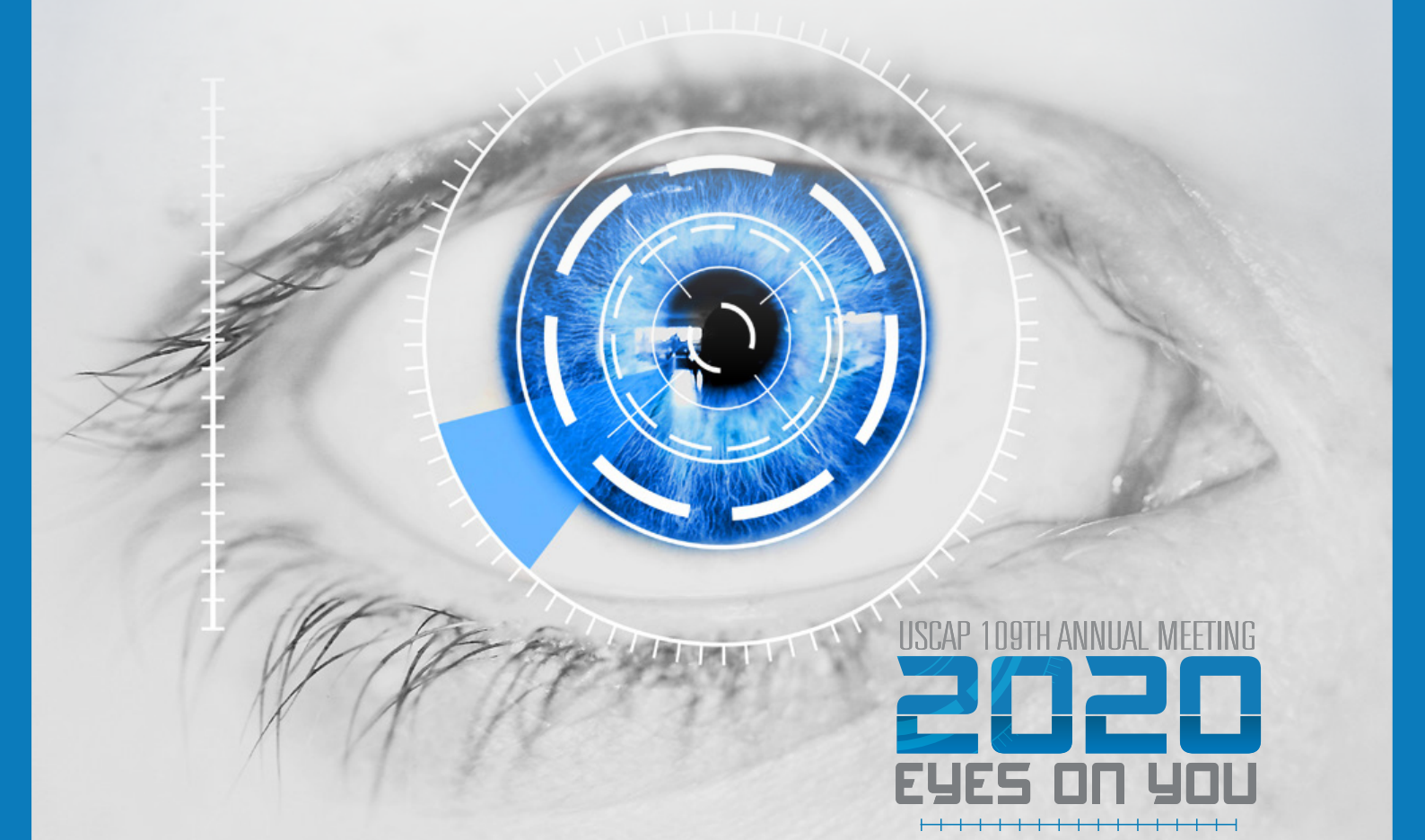

FEBRUARY 29-MARCH 5, 2020

LOS ANGELES CONVENTION CENTER
LOS ANGELES, CALIFORNIA

Published by
SPRINGER NATURE
www.ModernPathology.org

USCAP Creating a Better Pathologist
AN OFFICIAL JOURNAL OF THE UNITED STATES AND CANADIAN ACADEMY OF PATHOLOGY

EDUCATION COMMITTEE

Jason L. Hornick, Chair

Rhonda K. Yantiss, Chair, Abstract Review Board and Assignment Committee

Laura W. Lamps, Chair, CME Subcommittee

Steven D. Billings, Interactive Microscopy Subcommittee

Raja R. Seethala, Short Course Coordinator

Ilan Weinreb, Subcommittee for Unique Live Course Offerings

David B. Kaminsky (Ex-Officio)

Zubair Baloch
Daniel Brat
Ashley M. Cimino-Mathews
James R. Cook
Sarah Dry
William C. Faquin
Yuri Fedoriw
Karen Fritchie
Lakshmi Priya Kunju
Anna Marie Mulligan
Rish K. Pai
David Papke, Pathologist-in-Training
Vinita Parkash
Carlos Parra-Herran
Anil V. Parwani
Rajiv M. Patel
Deepa T. Patil
Lynette M. Sholl
Nicholas A. Zoumberos, Pathologist-in-Training

ABSTRACT REVIEW BOARD

Benjamin Adam
Narasimhan Agaram
Rouba Ali-Fehmi
Ghassan Allo
Isabel Alvarado-Cabrero
Catalina Amador
Roberto Barrios
Rohit Bhargava
Jennifer Boland
Alain Borczuk
Elena Brachtel
Marilyn Bui
Eric Burks
Shelley Caltharp
Barbara Centeno
Joanna Chan
Jennifer Chapman
Hui Chen
Beth Clark
James Conner
Alejandro Contreras
Claudiu Cotta
Jennifer Cotter
Sonika Dahiya
Farbod Darvishian
Jessica Davis
Heather Dawson
Elizabeth Demicco
Katie Dennis
Anand Dighe
Suzanne Dintzis
Michelle Downes
Andrew Evans
Michael Feely
Dennis Firchau
Gregory Fishbein
Andrew Folpe
Larissa Furtado
Billie Fyfe-Kirschner
Giovanna Giannico
Anthony Gill
Paula Ginter
Tamara Giorgadze
Purva Gopal
Anuradha Gopalan
Abha Goyal
Rondell Graham
Alejandro Gru
Nilesh Gupta
Mamta Gupta
Gillian Hale
Suntrea Hammer
Malini Harigopal
Douglas Hartman
John Higgins
Mai Hoang
Mojgan Hosseini
Aaron Huber
Peter Illei
Doina Ivan
Wei Jiang
Vickie Jo
Kirk Jones
Neerja Kambham
Chiah Sui Kao
Dipti Karamchandani
Darcy Kerr
Ashraf Khan
Francesca Khani
Rebecca King
Veronica Klepeis
Gregor Krings
Asangi Kumarapeli
Alvaro Laga
Steven Lagana
Keith Lai
Michael Lee
Cheng-Han Lee
Madelyn Lew
Zaibo Li
Faqian Li
Ying Li
Haiyan Liu
Xiuli Liu
Yen-Chun Liu
Lesley Lomo
Tamara Lotan
Anthony Magliocco
Kruti Maniar
Emily Mason
David McClintock
Bruce McManus
David Meredith
Anne Mills
Neda Moatamed
Sara Monaco
Atis Muehlenbachs
Bita Naini
Dianna Ng
Tony Ng
Michiya Nishino
Scott Owens
Jacqueline Parai
Yan Peng
Manju Prasad
Peter Pytel
Stephen Raab
Joseph Rabban
Stanley Radio
Emad Rakha
Preetha Ramalingam
Priya Rao
Robyn Reed
Michelle Reid
Natasha Rekhtman
Jordan Reynolds
Michael Rivera
Andres Roma
Avi Rosenberg
Esther Rossi
Peter Sadow
Steven Salvatore
Souzan Sanati
Anjali Saqi
Jeanne Shen
Jiaqi Shi
Gabriel Sica
Alexa Siddon
Deepika Sirohi
Kalliopi Siziopikou
Sara Szabo
Julie Teruya-Feldstein
Khin Thway
Rashmi Tondon
Jose Torrealba
Andrew Turk
Evi Vakiani
Christopher VandenBussche
Paul VanderLaan
Olga Weinberg
Sara Wobker
Shaofeng Yan
Anjana Yeldandi
Akihiko Yoshida
Gloria Young
Minghao Zhong
Yaolin Zhou
Hongfa Zhu
Debra Zynger

To cite abstracts in this publication, please use the following format: **Author A, Author B, Author C, et al. Abstract title (abs#). In "File Title."** ***Modern Pathology*** **2020; 33 (suppl 2): page#**

1503 Clinico-Histopathological Correlation of Leprosy- A Study from Tertiary Care Centre of Eastern Nepal

Purbesh Adhikari[1], Suchana Marahatta[1], Rajan Shah[1], Mona Dahal[1]
[1]*B.P. Koirala Institute of Health Sciences, Dharan, Nepal*

Disclosures: Purbesh Adhikari: *Primary Investigator*, B. P. Koirala Institute of Health Sciences; Purbesh Adhikari: *Primary Investigator*, B. P. Koirala Institute of Health Sciences; Mona Dahal: None

Background: Leprosy is a chronic infectious disabling disease resulting in disfigurement, deformity, stigma and disability. Large number of this debilitating disease is still reported from many countries of Asia, Africa and Latin- America.

Annual health report of our country does not reflect any substantial decrease in the number of the new leprosy patients and new case detection rate of leprosy i.e. New patient of leprosy in the year 2014/15 has decreased to only 3053 from 3157 in 2010/11. Similarly new case detection rate of leprosy has decreased to 11.01/100000 population in 2014/15 from 11.5/100000 population in 2010/11. This clearly indicates the ongoing transmission of the disease in this part of the world.

Exact tying of leprosy is sometimes clinically not possible because of its varied manifestations and complications. Histopathological examination is useful in classifying the cases accurately and is helpful in proper clinical management. Aim of the study was to perform clinicohistopathological correlation of leprosy and to classify leprosy according to Ridley Jopling classification.

Design: A cross-sectional study including clinically suspected cases of leprosy from four years of retrospective cases from August 2013-July 2017 and one year of prospective cases from August 2017-July 2018 was done.

Results: This study included total 162 skin biopsy samples of clinically suspected cases of leprosy. Male to female ratio was 1.13:1. Neurological involvement was present in 105 (64.8%) number of cases and nerve damage was seen in 93 (57.4%) number of cases. Most common skin lesion was plaque 94 (58%), followed by macule 26 (16%) and nodular lesion (11.1%). Leprosy was diagnosed in 158 of these skin biopsy samples on histopathological evaluation. 4 cases showed no histopathological agreement. Clinically most common diagnosis was borderline tuberculoid 110 (67.9%) which showed a histopathological agreement in 80 cases(72.7%). Second most common diagnosis clinically was lepromatous leprosy 30 (18.5%) which had a histopathological agreement in 23 cases (76.7%). Special stain for detection of Mycobacterium lepra was positive in 71 (44%) of cases.

Clinical Diagnosis Histopathological diagnosis

Types of Leprosy	Number of clinical leprosy patients (%)	TT	BT	BB	BL	LL	Histioid	IL	ENL	Others	Agreement	Percentage
TT	0	0	0	0	0	0	0	0	0	0	--	--
BT	110	0	80	6	8	5	0	9	0	2	80/110	72.7%
BB	0	0	0	0	0	0	0	0	0	0	--	--
BL	10	0	4	1	3	1	0		1	0	3/10	30%
LL	30	0	1	3	2	23	0	0	0	1	23/30	76.7%
Histioid	3	0	0	0	0	2	0	0	0	1	0/3	0%
IL	0	0	0	0	0	0	0	0	0	0	--	--
ENL	2	0	1	0	0	0	0	0	1	0	1/2	50%
Other diagnosis	7	0	2	0	1	4	0	0	0	0	--	--
Total	162	0	88	10	14	35	0	9	2	4		

Conclusions: Leprosy although considered to be eliminated from Nepal, is not eradicated and is prevalent in many areas. Although leprosy can be diagnosed clinically by evaluating number and types of skin lesions with nerve involvement and neurological deficit, combining clinical and histopathological diagnosis is important for proper management of patient.

1504 Cystic Neutrophilic Granulomatous Mastitis: Further Histologic Evidence Supporting an Infectious Etiology

Gabrielle Baker, Beth Israel Deaconess Medical Center, Boston, MA

Disclosures: Gabrielle Baker: None

Background: Cystic Neutrophilic Granulomatous Mastitis (CNGM) is an under-recognized pattern of granulomatous mastitis that is characterized by the presence of suppurative granulomatous inflammation with associated cystic spaces. The cystic spaces are frequently lined by neutrophils and are thought to represent sites of dissolved lipid; therefore, these may be referred to as suppurative lipogranulomas. The literature increasingly recognizes an association of coryneform bacteria, most notably *Corynebacterium spp*, with CNGM. Despite this association, an infectious etiology has not been broadly accepted. Previous studies have noted that the bacteria are typically scant and appear to be restricted to the cystic spaces within the suppurative lipogranulomatous inflammation. The purpose of this study was to review cases of CNGM with the specific aim of identifying putative early stage lesions and histologic alterations that might provide insight into the pathogenesis of CNGM.

Design: Cases of CNGM from a previously identified cohort (n=43) were reviewed to document the diverse histologic appearance of this disease process with particular attention to the adjacent breast parenchyma.

Results: As previously described, the characteristic finding was suppurative granulomatous inflammation; a subset of the granulomas was notable for cystic spaces, many of which were lined by a rim of neutrophils. Bacteria were identified within a subset of the cystic spaces and were typically scant. In many cases the suppurative lipogranulomatous infiltrate was a conspicuous component of the inflammatory process; however, in other cases the infiltrate was only nominally granulomatous.

Foci of granulomatous inflammation with associated neutrophils were identified within ducts and acini in multiple cases (Figure 1); foci of cystic dilatation were also identified within epithelial elements. Of particular interest, bacteria were occasionally identified within the small cystic spaces that were themselves present within ducts or acini (Figure 2). These findings are proposed to represent early stage lesions in the development of CNGM.

Figure 1 - 1504

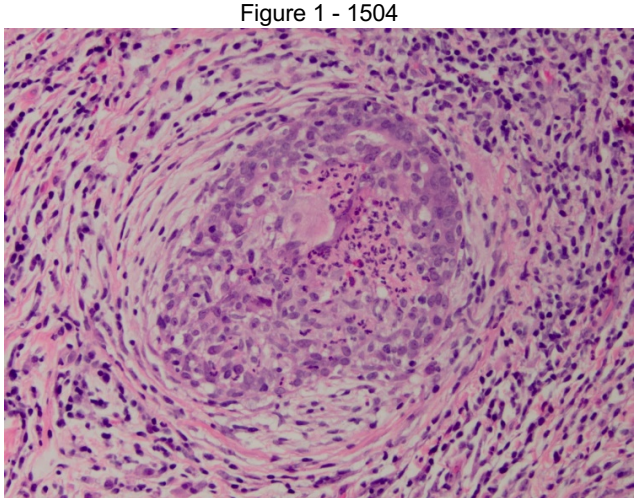

Figure 2 - 1504

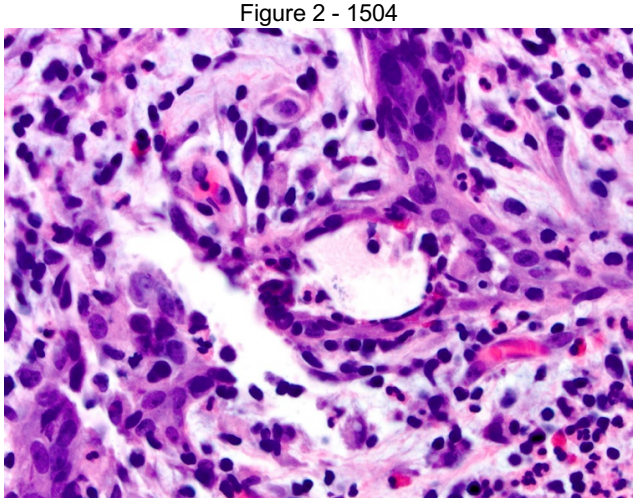

Conclusions: CNGM frequently recurs and is associated with significant morbidity. Assignment of an infectious etiology to CNGM has the potential to significantly impact the treatment algorithm for the disease. The observations described here provide insight into the pathogenesis of CNGM and provide further histologic evidence supporting an infectious etiology.

1505 Pathological Features and Differential Diagnosis of Chronic Intestinal Schistosomiasis

Lijun Cai[1], Shu-Yuan Xiao[1]
[1]*Department of Pathology, Zhongnan Hospital of Wuhan University, Wuhan, Hubei, China*

Disclosures: Lijun Cai: None; Shu-Yuan Xiao: None

Background: Chronic Schistosoma infestation may lead to misdiagnosis with inflammatory bowel disease. It is important to identify clinical and pathologic features that may facilitate the differential diagnosis.

Design: This retrospective study was conducted to review clinical, endoscopic, imaging and histological features of patients diagnosed as chronic schistosomiasis without other superimposed diseases, from November 2014 to August 2019 in our hospital.

Results: 30 biopsies and 6 resections from 36 patients were identified, including 20 males and 16 females, ranging from 29 to 79 years of age. The most common manifestations were abdominal pain, bloody stool, abdominal distention and weight loss with anemia. The lesions were mainly located in the rectum and/or left colon in 25 (69.4%) patients. Colonoscopy showed yellow granular hyperplasia and polyps in 14 (38.9%) and 17 (47.2%) cases, respectively; imaging demonstrated multiple spotty or linear calcifications in bowel wall in 5 (13.9%); stool examination of 4 patients were negative for Schistosoma ova. 4 patients were initially diagnosed as ulcerative colitis and 2 Crohn's disease (CD) clinically (misdiagnosis rate 16.7%). Microscopically, calcified or ruptured Schistosoma ova were unevenly distributed mainly in the submucosa, some accompanied by granulomatous reactions, multinucleated giant cells and various degrees of fibrosis. Of note, some sites of egg deposition lacked tissues responses completely, and some granulomas contained no ova in the initial sections. No pyloric gland metaplasia, cryptitis and crypt abscesses were found. Tissue eosinophilic counts were not significantly elevated in these cases, similar to the peripheral blood eosinophil count and percentage.

Figure 1 - 1505

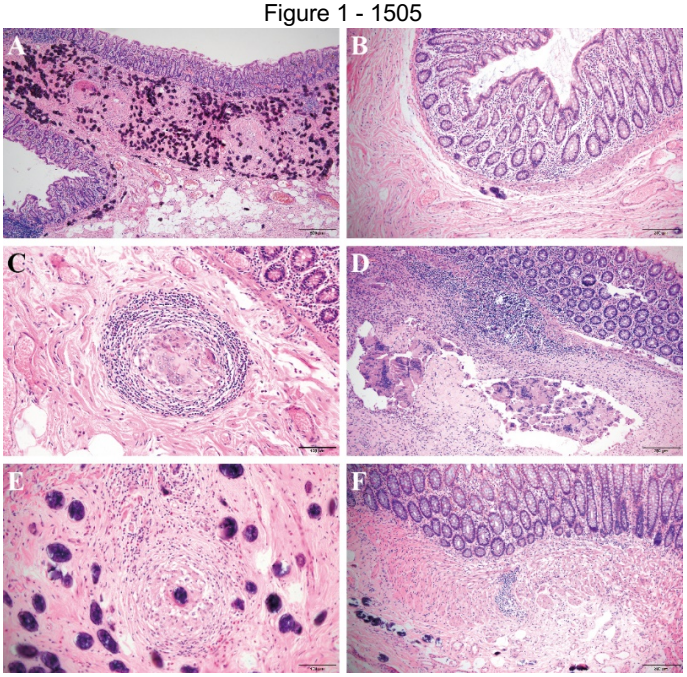

Figure 2 - 1505

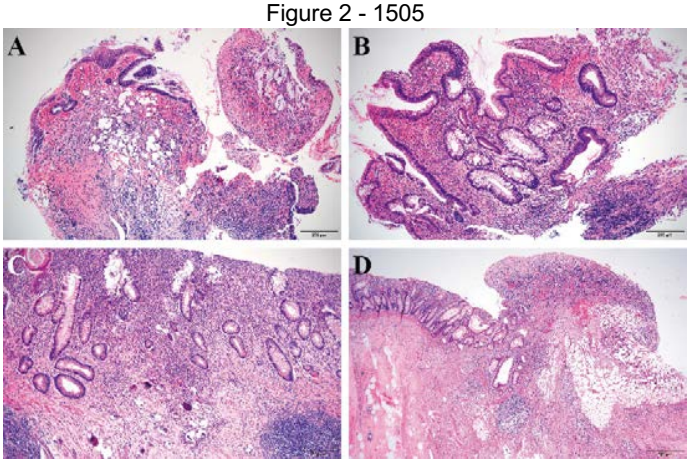

Conclusions: Clinical, endoscopic and imaging manifestations are not specific for chronic intestinal schistosomiasis. Stool examination, the peripheral blood eosinophil count and tissue eosinophilic quantification appear to be insensitive to identify chronic intestinal schistosomiasis. Awareness of this disease particularly in patients from endemic regions and proper patient demographic information should prompt rigorous search for parasitic eggs in colonoscopic biopsies to facilitate correct diagnosis, particularly in patients suspicious for IBD. Multiple levels of sectioning, particularly in tissue with otherwise typical granulomas, and multiple biopsies of the entire colon, will improve the diagnostic accuracy.

1506 Evaluation of the Performance Characteristics of the GenMark ePlex Rapid Blood Culture Identification Panels

Linlin Gao[1], Rachael Liesman[2]
[1]University of Kansas Medical Center, Overland Park, KS, [2]University of Kansas Medical Center, Kansas City, KS

Disclosures: Linlin Gao: None; Rachael Liesman: None

Background: Rapid and accurate diagnosis are essential to the prevention of morbidity and mortality associated with bacteremia and sepsis. Standard culture-based workflow requires 24 - 48 hours following a positive blood culture for identification and antimicrobial susceptibility testing of the etiologic agent. Molecular testing is a rapid and accurate method for the identification of bacteria from positive blood culture bottles and may provide preliminary susceptibility results based on the detection of resistance genes. The recently FDA-cleared GenMark ePlex Blood Culture Identification Gram-Positive (BCID-GP) and Gram-Negative (BCID-GN) panels are novel molecular assays for the identification of Gram-positive and Gram-negative bacteria from positive blood culture bottles.

Design: Positive blood culture bottles were tested by the ePlex system and standard-of-care methods. The first positive bottle per patient was tested and the bottle Gram stain was used to select the appropriate ePlex panel. ePlex results were compared to current laboratory practice. Following subculture to appropriate media, organisms were identified by MALDI-TOF MS and susceptibility testing was performed on a BD Phoenix automated instrument. Predicted inclusivity was determined by retrospectively evaluating the prevalence of organisms identified from positive blood culture bottles over a one-year period.

Results: In total, 112 positive blood culture samples were evaluated, using 67 Gram-positive panels and 45 Gram-negative panels. In 11 samples, the organism was not identified by the GenMark panel due to lack of target on the panel. Of the 101 valid results, the sensitivity of the ePlex panels was 100% for both Gram-positive bacteria (59/59) and Gram-negative bacteria (42/42). The specificity of the ePlex panels was 99.8% (1001/1003) for Gram-positive bacteria and 100% (672/672) for Gram-negative bacteria. The sensitivity of CTX-M gene detection by the BCID-GN panel was 87.5% (7/8) and specificity was 100% (20/20). The sensitivity and specificity of *mecA* and *vanA* gene detection were 100%. Predicted inclusivity was 91.6% for the BCID-GP and 96.5% for the BCID-GN.

Conclusions: The ePlex BCID-GP and BCID-GN panels demonstrated high sensitivity and specificity for the identification and prediction of antimicrobial susceptibility results from positive blood culture bottles. Results are available within 2 hours and both panels offer broad coverage of commonly detected organisms.

1507 Syphilitic Aortitis: Still a Challenge

Luiz Felipe Gonçalves[1], Lee I Ching[2], Carlos Otavio Goncalves[3], Daniella Vieira[4], Ariane Haagsma[5], Ana Carolina Rodrigues[1], Pietro Cantú[1], Pillar Venzon[2], Jéssica Lima[6], Renan Magri[7]
[1]Hospital Polydoro Ernani de São Thiago HU/UFSC, Florianópolis, SC, Brazil, [2]Universidade Federal de Santa Catarina, Florianópolis, SC, Brazil, [3]Medicina Diagnóstica São Lucas, Tubarao, SC, Brazil, [4]Hospital Polydoro Ernani de São Thiago HU/UFSC, São Jose, SC, Brazil, [5]Palhovßa, SC, Brazil, [6]Hospital Polydoro Ernani de São Thiago HU/UFSC, Itapema, SC, Brazil, [7]Universidade do Sul de Santa Catarina - UNISUL, Tubarão, SC, Brazil

Disclosures: Luiz Felipe Gonçalves: None; Lee I Ching: None; Carlos Otavio Goncalves: None; Daniella Vieira: None; Ariane Haagsma: None; Ana Carolina Rodrigues: None; Pietro Cantú: None; Pillar Venzon: None; Jéssica Lima: None; Renan Magri: None

Background: In Brazil, syphilis is an infectious disease that has been on the rise during the last few years. Between 2010 and June 2018, 479.730 cases of acquired syphilis were notified at the Brazilian Notifiable Grievance Information System (Sinan). Genital lesions are the most common ones to be diagnosed, but tertiary syphilis post significant challenges because of the uncommon sites it may appear.

Design: We present a case of a 62-year-old female from the south of Brazil who presented with symptoms of unstable angina and dyspnea. The angiotomography showed an aortic aneurysm. She underwent surgery and the aneurysm was for analysis with the diagnostic hypothesis of aortic tuberculosis. Histologic examination showed granulomatous pattern with central necrosis mainly with lymphocytes and plasma cells. The Ziehl-Nelseen stain for mycobacteria resulted negative. The Whartin-Starry stain and the immunohistochemistry with a polyclonal rabbit antibody to Treponema pallidum resulted positive for spirochetes. Her blood was tested with the Fluorescent Treponemal Antibody Absorption test (FTA-ABS test), which was reactive.

Results: Histological findings:

Figure 1: Granulomatous pattern in a aorta section.
Figure 2: A) Necrosis of the elastic fibres and connective tissue in the aortic media.
B and C) Identification of the spirochete by Immunohistochemistry and Whartin-Starry stain.

Figure 1 - 1507

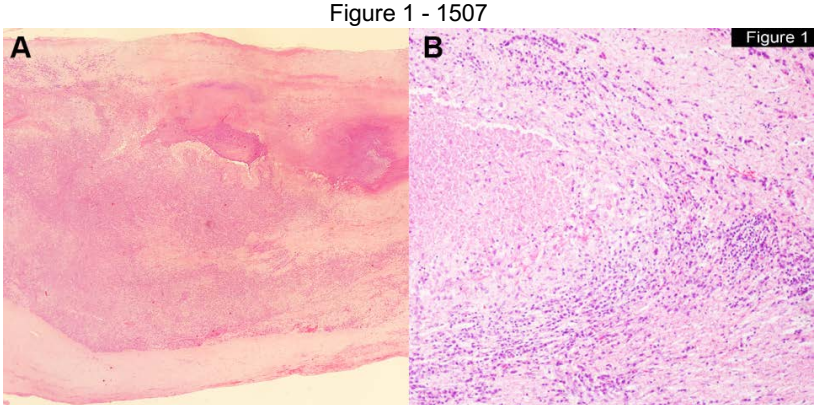

Figure 2 - 1507

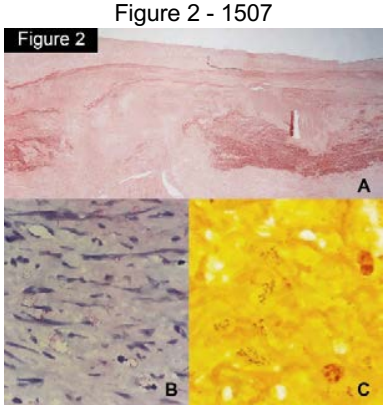

Conclusions: Following its reputation as the great imitator, syphilis can be hard to diagnose, especially in its tertiary stage. Receiving biopsies without the suspicion of syphilis is common and the pathologist should always be able to consider the possibility of tertiary syphilis.

1508 Effect of Microscope Magnification in Detection of Mycobacterium Tuberculosis Bacilli in Lymph Node Biopsies

Sumaiya Haddadi[1], Henry Mwakyoma[2]
[1]MUHAS, Dar es Salaam, Tanzania, [2]Muhimbili University of Health and Allied Sciences, Dar es Salaam, Tanzania

Disclosures: Sumaiya Haddadi: None

Background: Extrapulmonary TB (EPTB) is described as TB infection outside the pulmonary parenchyma as a result of hematogenous and lymphatic spread of the *Mycobacterium tuberculosis* bacilli. EPTB accounts for 20% of new cases of TB in Tanzania with several challenges in the diagnosis. The tissue biopsies with suggestive histomorphological features of TB on routine Haematoxylin and Eosin (H/E) stain further need to be stained with Ziehl Neelsen (ZN) stain and examined to detect acid fast bacilli (AFB). The highest magnification used in anatomical pathology unit to obtain detail cellular morphological features is x40 magnification and the same used to examine the ZN stained slides. In bacteriology, detection and appreciation of structural details of microorganisms is the main aim, x100 oil immersion magnification is used allowing for higher magnification with increased resolution. The main aim of this study was to observe any difference in detection of *Mycobacterium tuberculosis* bacilli in lymph node biopsies stained with ZN stain using x40 magnification and x100 oil immersion magnification.

Design: This was a retrospective cross-sectional study using archived lymph node biopsies retrieved over a 5-year period from the histopathology unit at MNH. FFPE blocks were subjected to microtomy and 2-micron thick sections were obtained. Sections were stained with H/E stain, reviewed and further stained with ZN stain. Slides were examined using LEICA DM750 microscope at x40 dry objective and x100 oil immersion magnification to detect the AFB. At x40 magnification the sections were reported positive and negative while at x100 oil immersion the positive sections were graded according to the number of bacilli present (IUATLD,2000).

Results: A total of 78 lymph node biopsies were reviewed and included in the study. The overall frequency of *Mycobacterium tuberculosis* bacilli in lymph node biopsies stained with ZN was 13 (16.7%). Among the 13 positive lymph node biopsies, 4 (30.8%) were detected with *Mycobacterium tuberculosis* bacilli at x40 magnification while at x100 oil immersion magnification *Mycobacterium tuberculosis* bacilli was detected in 9 (69.2%) more lymph node biopsies.

Table 1: Comparison of Mycobacterium tuberculosis bacilli detected at x40 and x100 oil immersion magnification in ZN stained lymph node biopsies

MAGNIFICATION POWER	POSITIVE N (%)
X40	4 (30.8)
X100 OIL IMMERSION	9 (69.2)
TOTAL	13 (100)

Figure 1 - 1508

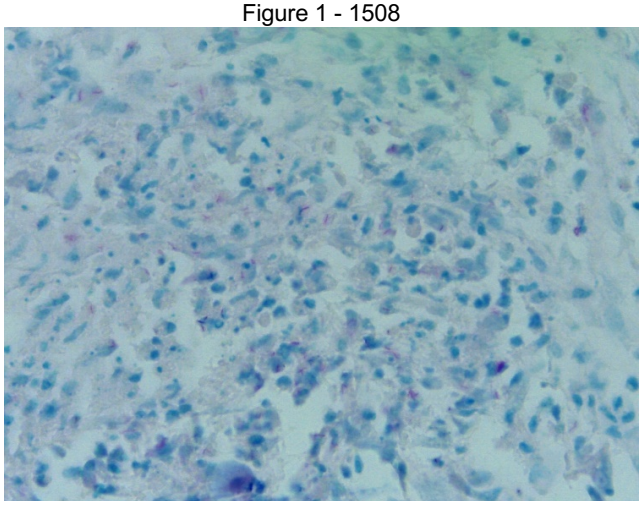

Figure 2 - 1508

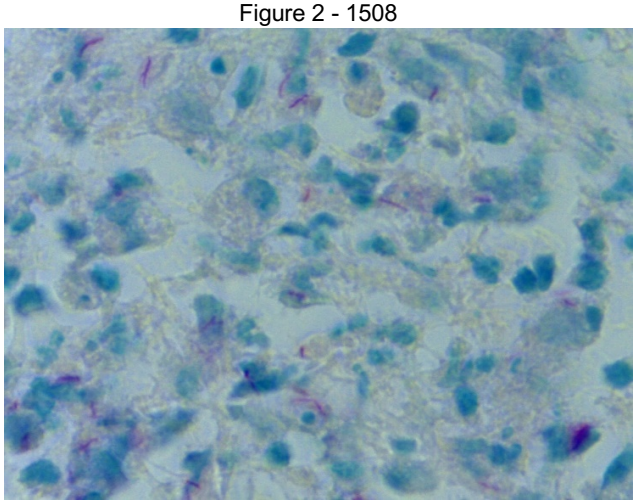

Conclusions: The Ziehl Neelsen stained sections should be examined using x100 oil immersion magnification to allow for improved detection of *Mycobacterium tuberculosis* bacilli and prevent false negative results.

1509 HPV Strain Characterization and Impact by Highly Active Antiretroviral Therapy (HAART) in HIV-Infected Anal Squamous Dysplasia and Carcinoma

Katrina Krogh[1], Sam Weinberg[1], Jie Liao[2], Guang-Yu Yang[2]
[1]McGaw Medical Center of Northwestern University, Chicago, IL, [2]Northwestern University, Chicago, IL

Disclosures: Katrina Krogh: None; Sam Weinberg: None; Jie Liao: None; Guang-Yu Yang: None

Background: High-risk human papillomavirus (HR-HPV) strains are causative agents of anal dysplasia and squamous cell carcinoma (SCC) with increased incidence in human immunodeficiency virus (HIV+) patients. Studies have consistently found higher frequencies of co-infection with multiple strains compared to HIV− patients. We previously showed that HAART could slow the progression of anal dysplasia. However, the prevalence of specific HPV strains and impact of HAART are unknown. We performed extensive DNA analysis of a large cohort of HIV+ patients with anal dysplasia and SCC.

Design: Over 300 dysplastic/cancerous anal biopsies from HIV+ patients were obtained. HAART-adherent and non-adherent patients were grouped and matched to HIV− controls. Tissue was graded from anal intraepithelial neoplasia-1 (AIN-1)–SCC. Concurrent viral loads (VL) and CD4 counts were obtained. Biopsies were analyzed for 17 HPV genotypes using qPCR: 12 high-risk (16, 18, 31, 33, 35, 39, 45, 51, 52, 56, 58, 59), three probable high-risk (53, 66, 68), one low-risk (6), and one undetermined (67).

Results: For HIV+/HAART+ patients, mean age was 47 years and 90% were male; average VL was 30 copies/mL and CD4 count was 573 cells/μL. For HIV+/HAART− patients, mean age was 41 years and 100% were male; average VL was 36,498 copies/mL and CD4 count was 186 cells/μL. For HIV− patients, mean age was 55 years and 37% were male. Most patients had >1 HR-HPV strain (64% HIV−, 78% HIV+/HAART+, 82% HIV+/HAART−). Many had ≥3 strains, with the highest prevalence in HIV+/HAART− (33% HIV−, 36% HIV+/HAART+, 72% HIV+/HAART−). HPV16 was the most prevalent strain (77% HIV+, 89% HIV−), followed by HPV67 (33% HIV−, 36% HIV+). Certain strains favored certain groups; HPV35 was common in HIV− (56%), uncommon in HIV+/HAART+ (27%), and absent in HIV+/HAART− groups. Other strains (33, 53, 45, 31) favored HIV+ patients. Interestingly, the number of diverse non-HPV16 strains was significantly higher in HIV+/HAART− (2.4±0.34) than HIV+/HAART+ (1.4±0.30) and HIV− (1.3±0.29) patients (P=0.04). Furthermore, AIN-1 and SCC cases had higher numbers of strains in the HIV+/HAART− group (3.7, 3.3) than in the HIV+/HAART+ (2.3, 2.3) and HIV− (1.5, 2.2) groups.

Conclusions: HAART significantly impacts populations of HR-HPV in HIV+ patients. HIV+/HAART+ and HIV− groups showed similar strain diversity, while HIV+/HAART− strain diversity was significantly increased. This implies that HAART not only eradicates HIV and restores immunity, but also reduces HPV infection diversity.

1510 Diagnosis of Acute Hepatitis E Virus Infection: A Case Series Focusing on Clinicopathologic Features with Salient Liver Biopsy Findings

Michelle Lin[1], Mary Schwartz[1], Suzanne Crumley[1], Sudha Kodali[1], Robert McFadden[1], Chukwuma Egwim[1], Victor Ankoma-Sey[1], David Victor[1], Mukul Divatia[1]
[1]Houston Methodist Hospital, Houston, TX

Disclosures: Michelle Lin: None; Mary Schwartz: None; Suzanne Crumley: None; David Victor: None; Mukul Divatia: None

Background: Hepatitis E virus (HEV) infection is a significant global health problem. In immunocompetent individuals, it usually follows a subclinical course or presents with acute hepatitis; but it may lead to chronic hepatitis or fulminant hepatic failure in immunocompromised patients and patients with underlying chronic liver disease. As it is infrequently biopsied, histopathologic features of acute HEV infection are not well-characterized in the literature.

Design: A retrospective institutional archival search for liver biopsies of HEV infection cases from 2009-19 was performed. Clinical data including age, sex, symptoms, travel history, liver function tests with autoimmune panel and infectious disease testing were recorded. H & E biopsy slides with trichrome and iron stains were reviewed.

Results: Liver biopsies (n=7) from 6 patients (5 females and 1 male, mean 62 years) were reviewed. Constitutional symptoms, abdominal pain and jaundice were noted in all except one asymptomatic case. All cases were seropositive for elevated HEV IgM (6) and/or IgG (3). Travel to Asia, an endemic region for HEV, was seen in 1 case and 5 cases were autochthonous. Three patients were immunosuppressed due to Crohn's disease (1), heart transplantation (1), and liver transplantation (1). Both transplant cases also had chronic hepatitis C infection. One patient had concomitant serum IgM positivity for cytomegalovirus. Titers for serum antinuclear antibody and anti-smooth muscle antibody were positive in two (1:320 and 1:160) and one (1:40) patients respectively. All biopsies showed acute hepatitis with lobular disarray, mild (3) to moderate (3) portal and lobular inflammation with focal bridging necrosis in one case. The inflammatory infiltrates comprised of lymphocytes, histiocytes, plasma cells, eosinophils and variable neutrophils with a mild bile ductular

reaction. Cholestasis was absent in 3 and focally present in 4 biopsies. Both cases with prior hepatitis C infection showed bridging fibrosis. Mild portal fibrosis was seen in 4 biopsies and 1 biopsy had no fibrosis.

Conclusions: Histopathologic diagnosis of HEV infection is challenging as the findings can be extremely variable and overlap with other causes of hepatitis, especially non-E viral infections, autoimmune hepatitis and drug induced liver injury. The histopathologic findings on biopsy, in correlation with clinical presentation, can raise a consideration of HEV infection which can be confirmed by serologic testing.

1511 Evaluation of (1,3)-β-D-Glucan Testing in Immunocompetent Patients at an Urban Safety Net Hospital and its Financial Burden on the Clinical Laboratory

Clare McCormick-Baw[1], Abby Lau[2], Julie Alexander[2], Sarath Nath[2], Nainesh Shah[3], Kavita Bhavan[2]
[1]UTSW, Dallas, TX, [2]UTSW Medical Center, Dallas, TX, [3]University of Texas Southwestern, Dallas, TX

Disclosures: Clare McCormick-Baw: None; Abby Lau: None; Sarath Nath: None; Nainesh Shah: None

Background: Diagnostic stewardship in healthcare is increasingly important. Testing that is expensive, has limited diagnostic accuracy, or has the potential of overuse can be a burden to the clinical laboratory. (1,3)-β-D-glucan testing is used to screen for invasive fungal infection, particularly in immunocompromised patients, but if its role is not well understood can lead to overuse. A reference lab performs testing at our institution; therefore, time to result ranges from 3-5 days. We aim to describe utilization of (1,3)-β-D-glucan testing at our institution among immunocompetent patients, where this test would have the most limited utility.

Design: Retrospective review of patient and laboratory data from the electronic medical record for (1,3)-β-D-glucan testing between 10/1/18-2/28/19 was performed. Analyzed data included patient demographics, indication for test, fungal cultures, and factors associated with false positive results. Financial analysis including the cost over the study period and an estimation of annual expenditure is included.

Results: 300 tests were ordered over the study period. 154 (51%) tests were ordered on immunocompromised patients and excluded from analysis. 146 (49%) tests were performed on immunocompetent patients. 18/146 (12%) tests were reported as positive, 106/146 (73%) were reported as negative, and 22/146 (15%) were indeterminate. 17/18 (94%) of patients had other testing for fungal infection; of those patients, 3/17 (18%) were positive. 98/106 (92%) of patients with a negative result had other fungal testing; of those patients, 15/98 (15%) were positive. 75/146 (51%) immunocompetent patients had ≥1 established risk factor for a false positive result. The cost of the test during the study period was estimated to be nearly $40,000 and projected to be approximately $95,000 annually.

Conclusions: (1,3)-β-D-glucan testing is ordered frequently at our institution to screen for invasive fungal infections. The most common indications for testing in immunocompetent patients were sepsis or concern for fungal pneumonia. Careful consideration must be given to the appropriateness of ordering this test because it has limited diagnostic accuracy, the risk of treating patients with potentially false positive results with unnecessary antifungal therapy, and there is significant cost to the hospital system. Improved education among clinicians about use of this test and research of clinical outcomes may help improve diagnostic stewardship efforts.

1512 Comparative Evaluation between Real-Time PCR Reaction Assay and Direct Immunofluorescence Antibody for Pneumocystis jirovecii

Melissa Mejia Bautista[1], Chao Qi[1]
[1]McGaw Medical Center of Northwestern University, Chicago, IL

Disclosures: Melissa Mejia Bautista: None; Chao Qi: None

Background: *Pneumocystis jirovecii* is an opportunistic pathogen responsible for Pneumocystis pneumonia (PCP) mainly in immunocompromised populations. Microscopic identification of P. jirovecii by staining respiratory samples with direct fluorescent labeled antibody (DFA) continues to be the most widely used method. However, detection of *P. jirovecii* is labor consuming and difficult to read. It also lacks sensibility for low fungal burdens, especially in non-HIV-infected patients. The *P. jirovecii* Assay from DiaSorin Molecular is a non-FDA approved real-time PCR assay allows for the detection of the organism in bronchoalveolar lavage (BAL), non-bronchoscopic BAL, induced sputum, and endotracheal specimens. In this study, the performance this assay was evaluated in comparison to *P. jirovecii* detection with DFA. The Microbiology laboratory currently performs *P. jirovecii* DFAs using the BioRad Monofluo™ *P. jirovecii* IFA Test Kit. This assay is potentially under consideration to replace the current test for its improved sensitivity, minimal hands-on time, and better turnaround time.

Design: A total of 149 pulmonary samples, including bronchoalveolar lavage (101), non-bronchoscopic BAL (26), induced sputum (20), and endotracheal clinical samples (2), that had been previously tested with BioRad Monofluo™ *Pneumocystis jirovecii* IFA Test Kit, were tested using the DiaSorin *P. jirovecii* Assay. PCR results were generated for 145 samples. Samples with discrepant results were sent to a reference lab for third party testing. Four samples were excluded from the analysis. PCR testing failed to produce result for 3 samples and third party testing was not performed due to insufficient sample volume

Results: 15 DFA positive samples were tested positive by PCR. 121 DFA negative samples were tested negative by PCR. 10 samples had discrepant results. 3 DFA positive samples were tested negative by PCR and 7 DFA negative samples were tested positive by PCR. The third party testing confirmed all the PCR results except for 1 negative PCR result. When comparing both test's results, 136 agreements (93.10% of the observations) were present. Overall, PCP DFA showed a sensitivity of 69.6% and a specificity of 99.2% whereas the PCR test showed a sensitivity of 95.7% and a specificity of 100%.

Conclusions: The higher sensitivity and specificity of the Pneumocystis jirovecii nucleic acid detection assay and its technical advantages make it a proper candidate for a future wider implementation in the laboratory and clinical setting.

1513 The Presence of Borrelia Burgdorferi in Periarticular Tissue of the Patients with Clinically Unsuspected Lyme Disease Stage III

Ondrej Ondic[1], Katerina Cerna[1], Jaroslav Voller[2], Reza Alaghehbandan[3]
[1]Biopticka laborator s.r.o., Pilsen, Czech Republic, [2]Biopticka laborator s.r.o., Plzeň, Czech Republic, [3]Royal Columbian Hospital, University of British Columbia, New Westminster, BC

Disclosures: Ondrej Ondic: None; Katerina Cerna: None; Jaroslav Voller: None; Reza Alaghehbandan: None

Background: Lyme disease is a multisystem infectious disorder caused by the spirochete, *Borrelia burgdorferi*. The infection occurs by ticks feeding on mammalian hosts, including humans. The distribution of the tick and spirochete is especially prevalent in mild climate areas with forests and large deer populations including central Europe. Chronic oligoarthritis is the hallmark of stage III disease which frequently goes undetected.

Design: This is a two-year retrospective study based on histology review and selected molecular-genetic testing of resected periarticular tissue examined at the Departement of Pathology serving the catchment area with high tick and *B.burgdorferi* prevalence.

Results: The studied population consisted of an index case and 117 tissue samples from patients operated on in 2017-2018. Upon the histology review, 53 cases with at least minimal lymphoplasmacytic infiltrate were selected for further genetic testing. The presence of *B. burgdorferi* DNA was confirmed in 2/53 cases (3,8 %). The most significant histologic features associated with the presence of *B.burgdorferi* were: perivascular lymphoplasmacytic infiltrate and more specifically intramural lymphocytic infiltrate paired with concentric smooth muscle vascular wall hyperplasia. Of interest, *B. burgdorferi* positive cases occurred in the elbow region of adult men (43 and 75 yr) with a personal history of long-standing epilepsy or persistent forearm skin erythematous induration respectively.

Conclusions: 1. The preliminary estimated incidence of *B. burgdorferi* associated tissue lesions in the endemic region (i.e. the Czech Republic) is 3,8 %. 2. In periarticular tissue, the perivascular lymphoplasmacytic infiltrate is a non-specific finding in relation to the presence of *B. burgdorferi.* 3. The presence of *B. burgdorferi* was specifically associated with the presence of vascular wall lymphocytes and smooth muscle vascular wall hyperplasia. 4. In endemic areas, Lyme disease should be considered when examining elbow periarticular tissue in men. 5. Molecular-genetic testing is useful in identifying *B. burgdorferi* in an excisional specimen.

1514 Post-Treatment Bacterial Endocarditis Mimicking Fungal Organisms: A Morphologic Comparison and Tips for Avoiding this Diagnostic Pitfall

David Pacheco[1], Morgan Killian[2], Jennifer Perone[1], Beilin Wang[1], Ping Ren[1], Abe DeAnda[1], Vicki Schnadig[3], Heather Stevenson-Lerner[1]
[1]University of Texas Medical Branch, Galveston, TX, [2]University of Texas Medical Branch, Fort Worth, TX, [3]University of Texas Medical Branch, Seabrook, TX

Disclosures: David Pacheco: None; Morgan Killian: None; Beilin Wang: None; Ping Ren: None; Abe DeAnda: None; Vicki Schnadig: None

Background: A 57-year-old male with aortic stenosis and previous aortic valve replacement presented with fever (38.8°C) and embolic strokes due to infectious endocarditis. Blood cultures were positive for methicillin-sensitive *Staphylococcus aureus* (MSSA) and treatment with ceftriaxone and vancomycin was initiated. Operative intervention showed extensive vegetations of the aortic valve with complete destruction of the left ventricular outflow tract. Samples were submitted to pathology and the patient expired.

Design: Histology of the aortic valve excision showed extensive extra- and intracellular (mainly within histiocytes) organisms with morphologic features similar to *Histoplasma* spp. (by H&E and GMS). No organisms were isolated by tissue culture. Paraffin blocks were sent to the Centers for Disease Control and Prevention (CDC). The index case was then compared to a case of confirmed *H. capsulatum* endocarditis and a case of typical untreated MSSA endocarditis.

Results: Immunohistochemistry and PCR performed at the CDC were positive for MSSA and negative for *H. capsulatum*. Histologically the index case had a fibrinous exudate with histiocytic inflammation, an absence of neutrophils, and abundant round organisms measuring ~ 2-3 um. In contrast, the case of typical untreated MSSA endocarditis showed a purulent exudate with neutrophils. Features of *H.*

capsulatum endocarditis were similar to the index case with a fibrinous exudate, histiocytic inflammation, and large intracellular organisms, except with budding rather than septae observed under oil immersion. The histology of bacterial endocarditis may change after treatment; organisms may appear larger and the tissue may lack neutrophils and contain mainly fibrin. Measuring size is crucial since bacteria are smaller (~ 1 micron) than *H. capsulatum* (~ 3-4 microns) and similar pathogenic fungi. Following antibiotic treatment, bacteria (including MSSA) may appear larger (2-7 times their normal size) and resemble fungi. GMS stains enhance their larger appearance due to accumulation of silver precipitate.

Conclusions: We compared an index case of treated MSSA to a typical untreated case of MSSA and a confirmed case of H. *capsulatum* endocarditis. Treated MSSA endocarditis may resemble *H.* capsulatum endocarditis. In order to avoid this diagnostic pitfall, pathologists must remember to carefully examine the morphology under oil immersion to determine organism size and characteristic features such as septae or budding.

1515 Next Generation Microbiologists: Effective Integration of Clinical, Anatomic, and Molecular Pathology

Alexander Pyden[1], Sanjat Kanjilal[2], Sankha Basu[1], Isaac Solomon[1]
[1]Brigham and Women's Hospital, Boston, MA, [2]Harvard Medical School, Boston, MA

Disclosures: Alexander Pyden: None; Sanjat Kanjilal: *Consultant*, PhAST Diagnostics; Sankha Basu: None; Isaac Solomon: None

Background: Interpretation of diagnostic testing for infectious diseases is often limited by the increasing subspecialization that occurs in anatomic, clinical, and molecular pathology. The field of medical microbiology is ideally positioned to overcome this challenge by integrating data generated in separate laboratories into a coherent message to treating clinicians. To achieve this goal, medical microbiology fellowship training should include extensive exposure to infectious disease pathology and molecular microbiology, in addition to the traditional microbiology laboratory curriculum.

Design: Over a 3-month period at a large academic medical center, all cases were identified requiring interpretation by a medical microbiology fellow, through requests from clinical infectious disease specialists, anatomic pathologists, and microbiology laboratorians. The diagnostic outcomes of these consultations were reviewed, including contributions of anatomic pathology slide review, culture results, and targeted or broad-spectrum molecular testing.

Results: Of the 162 cases managed by the fellow during this period, 78 requests were initiated by the treating clinicians, 53 by anatomic pathologists, and 31 from within the microbiology laboratory. Most cases (n=123, 76%) involved interpretation of microbiology data, half (n=84; 52%), review of pathology slides, and 20% (n=32) integration of molecular results. The most frequent consult was triage for molecular testing, of which 32/56 (57%) requests were approved. Of these, 12 (38%) were discordant with prior results (including 4 discords favored to be molecular false positives and 3 molecular false negatives). Fifty-three AP cases were reviewed as intradepartmental consults: 27 were requested for review of special stains, 15 for organism identification, 4 for question of infectious process, and 7 for interpretation of postmortem cultures. Roughly half contained an initial impression, with disagreement in 8/23 (35%) cases.

Figure 1 - 1515

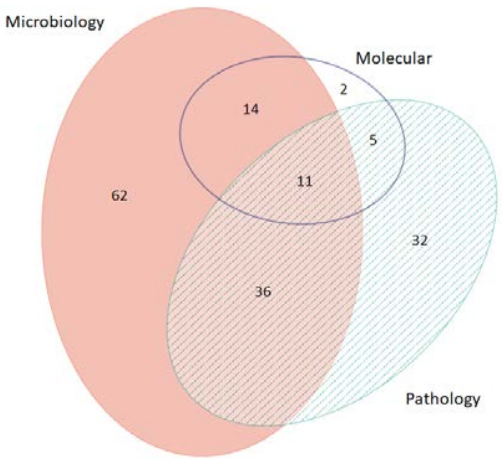

Conclusions: Through the coordination of a medical microbiology fellow, management of complex infectious disease cases has benefited from comprehensive review of culture results, histopathology, and molecular diagnostics. Unnecessary testing was prevented, and

diagnoses made that may have been missed without comprehensive review. Academic microbiology laboratories should embrace this critical role for professional consultation and provide trainees with opportunities to develop the skills to function effectively in this capacity.

1516 Correlation of Estimated Fungal Burden in Formalin-Fixed Paraffin-Embedded Tissue with Yield from Broad Range Fungal Sequencing

Krasimira Rozenova[1], Andrew Norgan[1], Robert Walchak[1], Nancy Wengenack[1]
[1]Mayo Clinic, Rochester, MN

Disclosures: Krasimira Rozenova: None; Andrew Norgan: None; Robert Walchak: None; Nancy Wengenack: None

Background: Identification of fungal organisms in human tissue is important for diagnostic purposes and patient management. Currently, fungal culture and direct histological visualization of fungal organisms are widely used, while serology and molecular methods have limited, but growing, applications. Fungal culture remains the gold standard for genus- and species-level identification, yet its utility is limited by slow (i.e., days-to-weeks) growth and fastidious organisms. Conversely, direct smears and histopathologic examination of formalin-fixed paraffin-embedded (FFPE) tissue are rapid methods, but morphologic identification of fungi at genus- or species-level can be challenging or impossible. By comparison, targeted molecular tests (e.g., PCR) provide rapid and specific identification of fungi, but are generally available only for a relatively small subset of pathogenic fungal organisms. Broad-range fungal sequencing (BRFS) is a promising unbiased and rapid molecular test with potential to provide a genus- or species-level identification of pathogenic fungi without a priori knowledge. This is particularly useful if infection is not suspected until after histopathologic examination, as unfixed tissue may no longer be available for culture. However, it is not well established whether visualization of fungal organisms on FFPE tissue is an important factor for BRFS-based identification.

Design: Our goal was to correlate the fungal organism burden and diagnostic yield of a BRFS approach. Forty-seven surgical pathology cases with reported filamentous microorganisms and correlating cultures were reviewed. The burden of fungal organisms in thirty two selected cases was estimated based on histopathological evaluation and designated as rare, low, medium or high (Fig.1). DNA from FFPE tissue was used for PCR amplification with two primer sets targeting the 28S and ITS regions of the 28S ribosome gene. Sanger sequencing of the PCR products was performed and the resulting nucleotide sequences were aligned (BLASTn) against the NCBI nucleotide collection database. Fungal identity of the top hit of each sequence was compared to identity determined by fungal culture.

Results: 13 out of 32 cases were successfully amplified and sequenced. The genus identification was determined in 12 cases from medium to high and only 1 case from rare to low fungal burden group (Fig.2).

Figure 1 - 1516

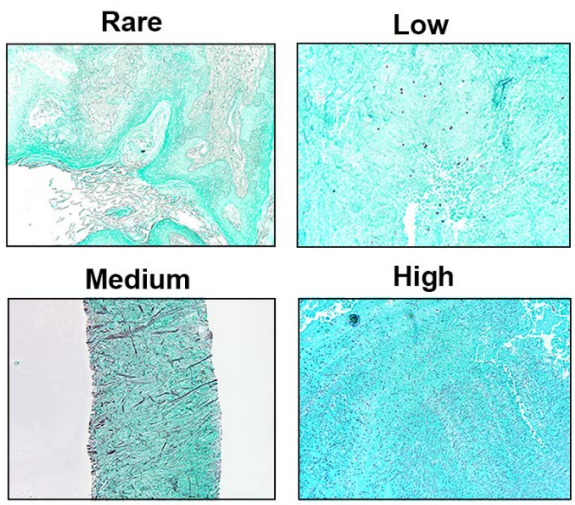

Fig.1 Fungal burden on GMS stained formalin-fixed paraffin-embedded tissue

Figure 2 - 1516

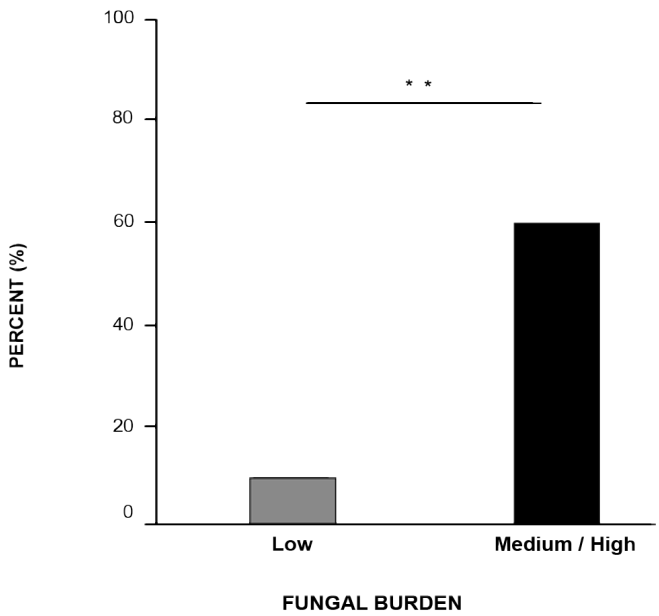

Fig.2. Genus-level identification by BRFS

Conclusions: Our study shows correlation between fungal burden and successful identification of fungal organism at the genus level by BRFS.

1517 Pancreatic Body Hydatid Cyst Linked to Pancreaticoduonectomy

Marco Serapião, Rio do Sul, Santa Catarina, Brazil

Disclosures: Marco Serapião: None

Background: Unilocular hydatid cyst is an infection caused by the larval stage of Echinococcus granulosus. Definitive hosts are canids (dog, wolf, hyena and others). The man functions as an intermediate host (among others), developing the larval stage (hydatid cyst). The liver and lung are the two most important sites of infection, but cysts can be found in several other organs. Occasionally compromises the pancreas. Due to its rarity and similarity with more common pancreatic cystic conditions, correct diagnosis of pancreatic hydatid cyst is usually challenging.

Design: 52-year-old female patient, currently residing in an *echinococcosis* endemic area, with a report of epigastric pain and gastric malfunction. Patient was then submitted to imaging examination. The ultrasound procedure revealed the presence of 5 cm pathogenic structure. After the surgical removal of the tissue and the macroscopic and microscopic analysis, the diagnosis was of a *hydatic cist.*

Results: Through macroscopic examination of the removed tissue, the 5 cm unilocular thick-walled cyst, with grainy inner surface, was found. Microscopic examination reveals a wall formed by three layers: the thick fibrous external (host reaction) involving a thinner laminated layer. Below this is a delicate layer of germinal epithelium containing calcareous corpuscles and multiple protoscoleces, allowing the diagnosis of hydatid cyst.

Figure 1 - 1517

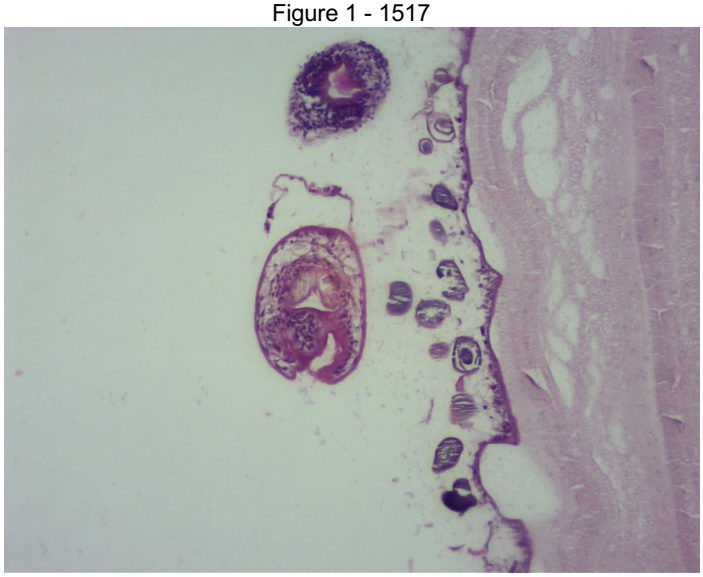

Figure 2 - 1517

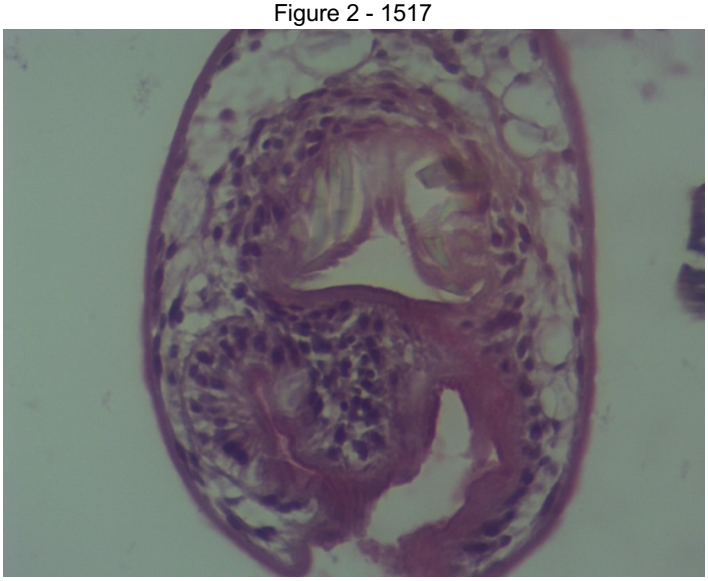

Conclusions: The presence of a cystic lesion located at the region of the pancreatic body detected by imaging, has led to a diagnostic possibility of pancreatic duct neoplasia with consequent radical surgical removal. Occasionally, infected individuals living in an endemic area migrate to a non-endemic area before symptoms occur, making it difficult to correctly diagnose because of a lack of epidemiological history. The report of the present case aims to alert other diagnostic possibilities, including parasitic etiologies, providing less invasive surgical therapeutic approaches.

1518 Performances of BioPlex 2200 Syphilis Assay and Architect Syphilis Immunoassay for Detection of Syphilis-Related Antibodies

Eric Tang[1], Diane Pytel-Parenteau[1], Kimberly Paiva[1], Shaolei Lu[2]
[1]Brown University School of Medicine, Providence, RI, [2]Alpert Medical School of Brown University, Providence, RI

Disclosures: Eric Tang: None; Diane Pytel-Parenteau: None; Shaolei Lu: None

Background: The BioPlex 2200 Syphilis IgG and Architect Syphilis TP assays are widely adopted in clinical practice for the first step of the reverse algorithm of serologic syphilis screening. The new BioPlex 2200 Syphilis Total with automated rapid plasma reagin (RPR) test is designed to perform the first two steps of the algorithm simultaneously. The performance of its Syphilis Total and automated RPR aspects need to be evaluated.

Design: We evaluated the diagnostic performances of the BioPlex Syphilis Total, BioPlex Syphilis IgG, Architect Syphilis TP, BioPlex automated RPR, and BD Macro-Vue RPR card on 293 samples in a tertiary medical center. Fujiribio Serodia TP-PA and patient chart review were used to resolve any discrepancies. Overall, positive, and negative agreement rates and Cohen's κ values were calculated to quantitate the comparison.

Results: Of all the 293 serum samples, 292 were examined by BioPlex Syphilis Total, 287 by BioPlex Syphilis IgG, 271 by Architect Syphilis TP, 282 by BioPlex RPR, and 283 by BD RPR. In comparison to TP-PA, BioPlex Syphilis Total obtained positive, negative, and overall rates of agreement of 96.5%, 100.0%, and 97.9%, respectively; Architect Syphilis TP obtained corresponding rates of 100.0%, 96.7%, and 98.5%; and BioPlex Syphilis IgG obtained corresponding rates of 100.0%, 80.8%, and 91.6%. All three assays had excellent concordance with the TP-PA result. We then analyzed the concordance between BioPlex RPR and BD RPR based on assay positivity and titer values. Out of 280 samples tested by both RPRs, there were 32 discordant samples. Of those, 28 of them were BD RPR +/BioPlex RPR- and 4 were BD RPR-/BioPlex RPR+. 72.3% of the samples had the same titer; ±1 titer agreement rate was 86%; and ±2 titer agreement rate was 95%. A logarithmic plot of the titers revealed an overall lower trend of BioPlex RPR comparing to BD RPR. 9 out of 24 cases of 1:1 positive by BD RPR are considered by BioPlex RPR as negative, 12 out of 26 cases of 1:2 as negative, 6 out of 17 cases of 1:4 as negative and 1 out of 14 cases of 1:8 as negative. Patient chart review showed that these were known syphilis patients and all had possibility of active infection at time of blood sampling.

Conclusions: Our results demonstrated that all three syphilis antibody assays had excellent performances compared to the TP-PA result. In addition, they suggest that the BioPlex RPR underdetected active syphilis and its implementation should depend on the patient population that the laboratory serves.

1519 Detection of Corynebacterium kroppenstedtii (Ck) in Granulomatous Lobular Mastitis (GLM) Using Real-Time PCR and Sanger Sequencing on Formalin-Fixed Paraffin-Embedded (FFPE) Tissues

Hamza Tariq[1], Menon Preethi[1], Hongxin Fan[2], Kumari Vadlamudi[3], Sri Lakshmi Pandeswara[1], Alia Nazarullah[1], Daniel Mais[4]
[1]The University of Texas Health Science Center at San Antonio, San Antonio, TX, [2]San Antonio, TX, [3]University of Texas Health Science Center at San Antonio, San Antonio, TX, [4]UT Health San Antonio, San Antonio, TX

Disclosures: Hamza Tariq: None; Kumari Vadlamudi: None; Sri Lakshmi Pandeswara: None; Alia Nazarullah: None; Daniel Mais: None

Background: Granulomatous Lobular Mastitis (GLM) is an inflammatory breast disease characterized by non-necrotizing lobulocentric granulomatous inflammation. Associations between GLM and *Corynebacterium* species (mainly Ck) have been reported since 2002, but accurately identifying Ck in clinical samples is challenging. We analyzed FFPE tissues from 56 cases of GLM by sequential DNA amplification and sequencing in order to assess the rate of Ck detection by this method.

Design: We retrospectively identified 56 cases of GLM over a 10-year period, in addition to 8 cases of non-granulomatous breast abscess included as controls. Patient demographics, clinical presentation, radiographic findings, histologic pattern, Gram stain, and culture information were reviewed and are summarized in Table 1.

DNA was extracted from FFPE tissue using the EZ1 DNA Tissue Kit (Qiagen), and amplified by SYBR real-time PCR with primers specifically targeting the Ck 16S rRNA gene region (primers cited from Fujii M et al. 2018). Ck PCR positive samples were Sanger sequenced using BigDye Terminator Cycle Sequencing Kit (Thermo Fisher Scientific) on the ABI3130xl Genetic Analyzer. Obtained sequences were analyzed using DNASTAR Lasergene 10 software (DNASTAR, Inc). Resulting sequences were queried in the GenBank database using BLASTn, and results with the highest alignment scores were reported.

Results: Ck 16S rRNA SYBR real-time PCR was positive on FFPE tissues from 42/56 (75%) GLM cases, while 14/56 (25%) GLM and 8 control cases were negative for Ck PCR. Clean sequences with read length of 102-137 base pairs were obtained from 41/42 PCR positive GLM cases, and GenBank search indicated 99% or 100% sequence similarities to Ck genome for these 41 GLM.

Clinical Data		**Pathology findings**	
Age range	17 – 81 years, mean 36.5 years	Cases with lobulocentric granulomas (figure 1a)	53.5 %
Ethnicity	Hispanic - 78.5 % Caucasian - 16.0 % Other - 5.5 %	Cases with diffuse granulomas (figure 1b)	46.5 %

Presentation	Painful mass – 76.7 % Painless mass – 10.3 % Other symptoms – 13 %	Cases with Cystic Neutrophilic Granulomatous Mastitis (CNGM) pattern (figure 2a)	50 %
Imaging	BIRADS III – 21.4 % BIRADS IV – 48.2 % BIRADS V – 5.3 % Unknown – 25.1 %	Gram stain positive cases (figure 2b)	17.8 %
		Cases with *Diphtheroids* (*Coryneforms) positive cultures*	19.6 %

Table 1 – Summary of demographics, clinical presentation, radiographic findings, histologic pattern, Gram stain and cultures

Figure 1 - 1519

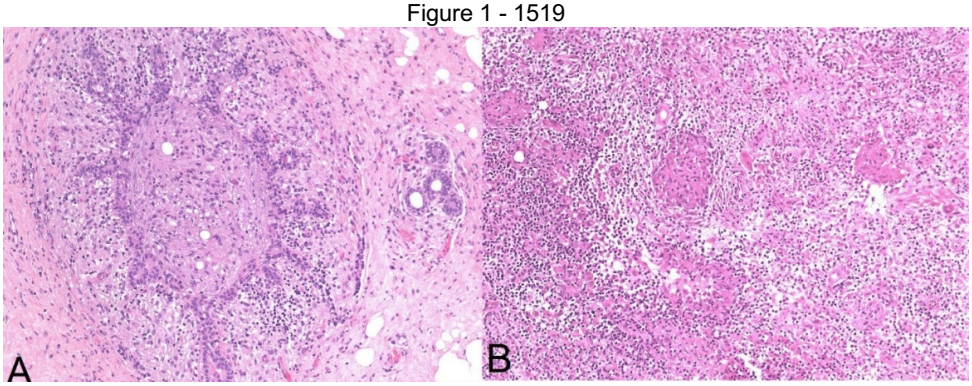

Figure 2 - 1519

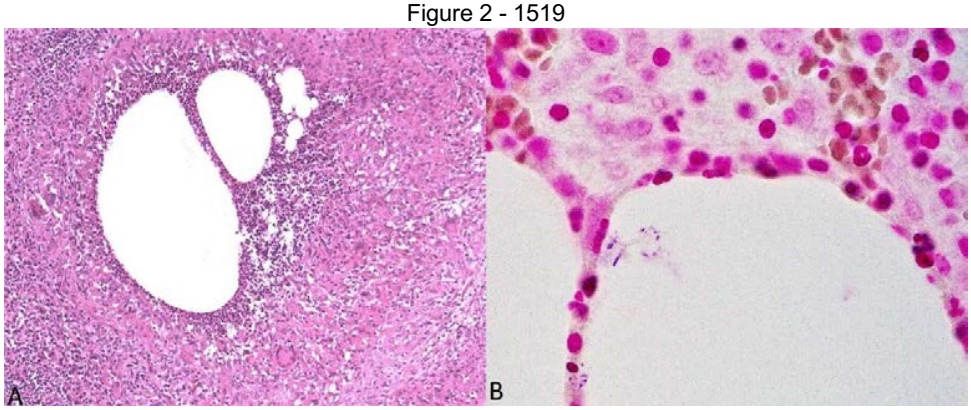

Conclusions: Our study demonstrated that Ck is highly prevalent in GLM proven by detection of Ck DNA in 3/4th GLM FFPE tissues by real-time PCR, and the presence of Ck was also confirmed by Sanger sequencing. These molecular detection methods can be performed on routinely processed FFPE samples and serve as useful diagnostic tools for the identification of Ck in GLM.

1520 Anaplasmosis: Diagnostic Clues for an Elusive Emerging Infection

Patricia Tsang, Geisinger, Kingston, PA

Disclosures: Patricia Tsang: None

Background: Anaplasmosis, a tickborne bacterial illness, has been steadily increasing in incidence since it first became recognized as a human disease in the U.S. in the mid-1990s. As an emerging infection, the diagnosis of anaplasmosis can be elusive for clinicians and pathologists. This study contributes to our understanding of this increasingly important diagnosis by retrospectively reviewing the laboratory and microscopic characteristics of confirmed cases of Anaplasma.

Design: A total of 28 consecutive cases of confirmed Anaplasma was collected from our institution based on positive molecular PCR results in the summer of 2019. A retrospective chart review, including any patient history of tick bites, relevant laboratory values (e.g. CBC and chemistry values in our institutional sepsis protocol) and peripheral blood smear findings, was performed. The results were deidentified, summarized and trended. Peripheral blood smears on these patients around the time of diagnosis were reviewed.

Results: In the peak tick season of June, July and August, our institution experienced a positive PCR rate of 21% for Anaplasma. Of the 28 consecutive patients with confirmed anaplasmosis, 50% had a documented history of a tick bite that ranged from 5 days to 21 days from initial clinical presentation. Patients typically presented to the emergency room with fever of unknown origin and signs of sepsis. The majority (n=18 or 64%) presented with a low absolute neutrophil count while 18% showed an elevated count (range=0.1 to 15.8 K/uL). Most of the patients (82%) experienced worsening thrombocytopenia, averaging 103 K/uL and ranging from 30 to 240 K/uL at initial presentation. All cases showed elevated procalcitonin levels, averaging 3.2 ng/mL. Of the 20 cases with pathologist review of peripheral blood smears prior to the positive PCR results, only 2 (10%) were provided with a clinical suspicion of organisms and 5 (25%) were correctly diagnosed based on the recognition of neutrophilic intracytoplasmic morulae.

Figure 1 - 1520

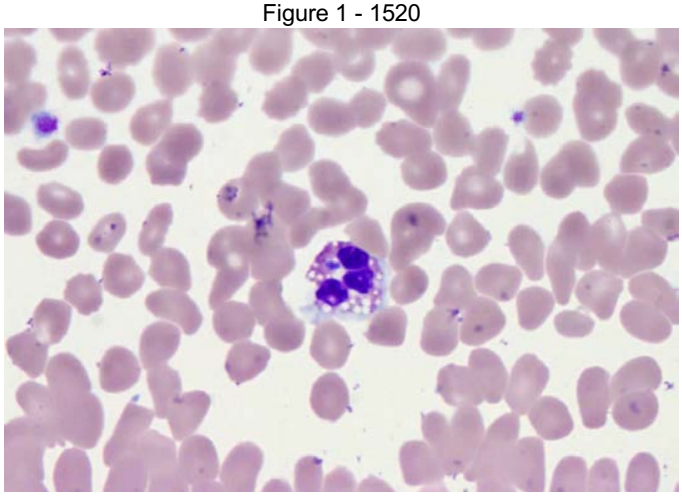

Conclusions: A high index of suspicion for anaplasmosis is important for correct patient diagnosis even without a history of tick bites. This study has shed light on the clinical, laboratory and blood smear characteristics of anaplasmosis as an elusive emerging infection that had taken up to 3 weeks for correct diagnosis. Anaplasmosis is associated with neutropenia, thrombocytopenia, elevated procalcitonin and intracytoplasmic morulae on blood smear.

1521 RNA- In Situ Hybridization on Paraffin Embedded Tissue can Distinguish Mycobacterium Tuberculosis Complex from Non-Tuberculous Mycobacteria

Julian Villalba[1], John Branda[2], Miguel Rivera[3], David Ting[3], Vikram Deshpande[2], Niyati Desai[4]
[1]Boston, MA, [2]Massachusetts General Hospital, Boston, MA, [3]Massachusetts General Hospital, Charlestown, MA, [4]Massachusetts General Hospital, Quincy, MA

Disclosures: Julian Villalba: None; John Branda: *Consultant*, Roche Diagnostics; *Consultant*, DiaSorin Inc.; *Consultant*, T2 BioSystems; Miguel Rivera: *Grant or Research Support*, ACD (Advanced Cell Diagnostics); David Ting: *Primary Investigator*, ACD-Biotechne; Vikram Deshpande: *Grant or Research Support*, Advanced Cell Diagnostics; *Advisory Board Member*, Viela; *Grant or Research Support*, Agios Pharmaceuticals; Niyati Desai: None

Background: Tuberculosis (TB) is the world's deadliest infectious disease. A WHO consensus statement has called for new non-sputum diagnostics. Interpretation of acid fast bacilli (AFB) on Ziehl-Neelsen (ZN) stain used to visualize mycobacteria in Formalin-Fixed Paraffin Embedded (FFPE) tissue, can be challenging, time-consuming, and does not distinguish between M.TB complex (MTB) and non-tuberculous mycobacteria (NTM); an essential distinction for appropriate clinical management. We assessed the diagnostic accuracy of RNA-in situ hybridization(ISH) probes to distinguish MTB from NTM in FFPE tissue.

Design: We retrospectively assessed biobanked FFPE tissue collected at our institution from patients with culture-proven mycobacterial disease(MTB/NTM). The cohort included a series of 15 mycobacterial infections(10 MTB and 5 NTM) with simultaneous AFB stain and mycobacterial culture performed on the same sample as RNA in situ hybridization. We used 2 RNAscope RNA ISH probes: 1) probe specific for MTB, 2) probe designed to hybridize to both MTB and NTM ("combination probe"). The MTB probe targets 23SrRNA while the combination probe targets 16SrRNA. Slides were evaluated under 100X oil immersion lens until bacilli were found or the whole section was scanned. Time spent on slide evaluation was recorded. We evaluated the specificity of the assay using normal tissue(n= 120) as well as 7 biopsies from patients with non-tuberculous infectious and granulomatous diseases.

Results: The mean ages for MTB and NTM cases were 60 and 28 years, respectively. The cohort of tuberculous infections included specimens from 5 lymph node, 6 lungs,1 liver, 1 heart, 1 skin, and 1 intestine. Most cases (MTB:90%; NTM:80%) showed necrosis and/or granulomas on histology. Rod-like, beaded organisms were identified by the ISH probes in 4 cases that were also AFB-positive; the remaining cases were negative on both stains. Among the 4 positive cases, ISH could distinguish the 2 patients with MTB from the 2 with NTM. Organisms were detected sooner with ISH (mean=5.55 mins) than with ZN (mean=14.93 mins) (p=0.0034). All 7 samples of patients with infectious disease as well as histologically unremarkable tissue were negative and neither nonspecific background nor rod-like organisms were identified.

	TB positive (n=10)	NTM positive (n=5)	Other infectious diseases	Normal tissue
MTB probe	2/10	0/5	0/7	0/120
MTB and NTM probe (combination probe)	2/10	2/5	0/7	0/120
ZN staining	2/10	2/5	-	-

* Organisms on ISH were identified only in cases that were also positive on ZN stain.

Conclusions: The sensitivity of ZN stain and ISH were equivalent in our study. ISH with species specific probes can distinguish MTC from NTB. The ISH platform reduces the time required to identify mycobacterial organisms on FFPE tissues.